Small Molecule Therapeutics

Molecular Cancer Therapeutics

The CREB-Binding Protein Inhibitor ICG-001 Suppresses Pancreatic Cancer Growth

Michael D. Arensman[1], Donatello Telesca[2], Anna R. Lay[1], Kathleen M. Kershaw[1], Nanping Wu[3], Timothy R. Donahue[3], and David W. Dawson[1,4]

Abstract

Pancreatic ductal adenocarcinoma (PDAC) is a highly lethal cancer due in part to a lack of highly robust cytotoxic or molecular-based therapies. Recent studies investigating ligand-mediated Wnt/β-catenin signaling have highlighted its importance in pancreatic cancer initiation and progression, as well as its potential as a therapeutic target in PDAC. The small-molecule ICG-001 binds cAMP-responsive element binding (CREB)-binding protein (CBP) to disrupt its interaction with β-catenin and inhibit CBP function as a coactivator of Wnt/β-catenin–mediated transcription. Given its ability to inhibit Wnt/β-catenin–mediated transcription *in vitro* and *in vivo*, as well as its efficacy in preclinical models of colorectal cancer and other Wnt-driven diseases, we examined ICG-001 and its potential role as a therapeutic in PDAC. ICG-001 alone significantly inhibited anchorage-dependent and -independent growth of multiple PDAC lines, and augmented *in vitro* growth inhibition when used in combination with gemcitabine. ICG-001 had only variable modest effects on PDAC apoptosis and instead mediated PDAC growth inhibition primarily through robust induction of G_1 cell-cycle arrest. These effects, however, seemed decoupled from its inhibition of Wnt/β-catenin–mediated transcription. DNA microarrays performed on PDAC cells in the context of ICG-001 treatment revealed ICG-001 altered the expression of several genes with well-established roles in DNA replication and cell-cycle progression, including direct actions on *SKP2* and *CDKN1A*. ICG-001 also significantly prolonged survival in an *in vivo* orthotopic xenograft model of PDAC, indicating ICG-001 or derived compounds that disrupt CBP activity are potentially useful small-molecule therapeutics for pancreatic cancer. *Mol Cancer Ther; 13(10); 2303–14. ©2014 AACR.*

Introduction

Pancreatic ductal adenocarcinoma (PDAC) is among the deadliest of cancers, with an overall 5-year survival rate of approximately 6% (1). PDAC is difficult to treat because it frequently presents at an advanced, nonoperative stage and is highly resistant to cytotoxic or targeted molecular therapy (2). Although our understanding of the molecular and cellular basis of PDAC continues to expand, present therapeutic options remain limited and offer only modest survival benefits for most patients.

Wnt/β-catenin signaling is a critical developmental signaling pathway whose dysregulation is strongly implicated in the pathogenesis of many types of cancers (3). Canonical mutations in *CTNNB1, APC*, and *AXIN* that lead to constitutive hyperactivation of the pathway occur only infrequently in PDAC (4, 5). Nevertheless, perturbations in the timing, context, and strength of Wnt/β-catenin signaling can promote the development and progression of PDAC (4, 5). Ligand-mediated Wnt/β-catenin signaling is essential for pancreatic cancer initiation and progression (6) and has been linked to aggressive tumor behavior (7). Wnt pathway activation as detected by nuclear and/or cytoplasmic accumulation of β-catenin is observed in 10% to 65% of pancreatic intraepithelial neoplasia (PanIN; refs. 8, 9), increasing with higher PanIN grade and invasive PDAC (10). Genetic or pharmacologic inhibition of various steps in the Wnt pathway has also been shown to prevent *in vitro* (7, 9, 10) and *in vivo* tumor growth (6, 10–13), implicating Wnt signaling as a therapeutic target in PDAC.

Although previously plagued by poor *in vivo* pharmacokinetics, several novel Wnt/β-catenin inhibitors have demonstrable *in vivo* activity and are now in various stages of preclinical or early clinical development. These include naturally occurring compounds, small-molecule inhibitors, blocking antibodies, and peptide antagonists

[1]Department of Pathology and Laboratory Medicine, David Geffen School of Medicine at UCLA, Los Angeles, California. [2] Department of Biostatistics, David Geffen School of Medicine at UCLA, Los Angeles, California. [3]Deparment of Surgery, David Geffen School of Medicine at UCLA, Los Angeles, California. [4]Jonsson Comprehensive Cancer Center, David Geffen School of Medicine at UCLA, Los Angeles, California.

Note: Supplementary data for this article are available at Molecular Cancer Therapeutics Online (http://mct.aacrjournals.org/).

Corresponding Author: David W. Dawson, David Geffen School of Medicine at UCLA, Mail Code 173216, 10833 Le Conte Avenue, Los Angeles, CA 90095-1732. Phone: 310-267-2799; Fax: 310-267-2058; E-mail: ddawson@mednet.ucla.edu

doi: 10.1158/1535-7163.MCT-13-1005

©2014 American Association for Cancer Research.

Downloaded from http://aacrjournals.org/mct/article-pdf/13/10/2303/2327082/2303.pdf by guest on 12 February 2025

(5, 14, 15). ICG-001 was identified in a screen of small molecules that inhibited Wnt/β-catenin transcriptional activity in a colorectal cancer cell line (16). ICG-001 selectively blocks the interaction of β-catenin with its transcriptional coactivator cAMP-responsive element binding (CREB)-binding protein (CBP) without disrupting β-catenin interaction with highly homologous p300. One significant effect ascribed to ICG-001 and its disruption of Wnt/β-catenin transcription is decreased expression of the apoptosis inhibitor *BIRC5* (aka survivin protein), which leads to activation of caspase-3/7–mediated apoptosis (16–19). ICG-001 was first shown to slow colorectal cancer xenograft growth and intestinal polyp formation in the Apc^{min} mouse model (16) and has been subsequently shown to have *in vivo* efficacy in other Wnt-driven disease models, including rodent models of pulmonary fibrosis (20), renal interstitial fibrosis (21), acute lymphoblastic leukemia (22), chronic myocardial infarction (23), dermal fibrosis (24), and salivary tumorigenesis (25). The ICG-001–derived compound PRI-724 is now under investigation as a Wnt inhibitor in early-phase clinical trials for advanced solid tumors (NCT01302405) and myeloid malignancies (NCT01606579; ref. 26).

Given the importance of Wnt signaling in pancreatic carcinogenesis, we have now explored therapeutic potential and mechanism of action of ICG-001 in PDAC. ICG-001 significantly inhibited *in vitro* and *in vivo* PDAC growth by inducing G_1 cell-cycle arrest through effects that were largely decoupled from its activity as a Wnt inhibitor. Instead, ICG-001 seemed to more broadly affect CBP function as a cotranscriptional activator, directly and indirectly perturbing the expression of numerous genes with key roles in cell-cycle progression.

Materials and Methods

Cell lines and reagents

All cell lines were cultured as previously described (7). AsPC-1, MiaPaCa-2, and PANC-1 were obtained in 2005 from the ATCC (Rockville, MD). L3.6pl was obtained in 2010 from Hong Wu (UCLA). The cell lines have not been subsequently authenticated since receipt. ICG-001 was purchased from Selleck Chem and gemcitabine was kindly provided by Timothy Donahue (UCLA). Wnt3a and L-cell conditioned media were prepared as previously described (7).

Cell growth, proliferation, and apoptosis assays

MTT cell viability assays (ATCC) were carried out per the manufacturer's instructions at initial plating of 5,000 (AsPC-1 and L3.6pl) or 3,000 (MiaPaCa-2 and PANC-1) cells per well in 96-well plates. Soft agar assays were performed as previously described (7) in 48-well format. Media and drug were replenished once every 3 to 4 days. For cell-cycle analysis, treated cells were stained using hypotonic DNA staining buffer: 0.1 mg/mL propidium iodide (PI; Calbiochem), 20 μg/mL RNaseA, 1 mg/mL sodium citrate, and 0.3% Triton X-100. Flow cytometry analysis was performed in the UCLA Flow Cytometry Core using a Becton Dickinson FACSCalibur cytometer and using ModFit LT v3.1 software. Annexin-V–PI flow cytometry analysis was performed with Cellquest v3.3 software using an Annexin V FITC Apoptosis Detection Kit (BD Biosciences).

Orthotopic xenograft tumor assay

Animal work was performed with oversight by the UCLA Division of Laboratory Animal Medicine and approval from the UCLA Animal Research Committee. Orthotopic tumors were established by injecting 5×10^5 AsPC-1 cells suspended in 50% Matrigel (BD Biosciences)/RPMI into surgically exposed pancreatic tails of 6-week-old female athymic nude mice (Charles River) as previously described (27). Intraperitoneal drug injections were begun 10 days after tumor cell injections in animals randomized to four treatment arms: vehicle alone (20% PEG300, 5% solutol, 3.75% dextrose, 1% DMSO in PBS; $n = 12$); ICG-001 (5 mg/kg 6 days/week; $n = 12$); gemcitabine (25 mg/kg 2 days/week; $n = 11$); or ICG-001 + gemcitabine ($n = 12$). Treatment was for 8 weeks and then discontinued for the remainder of the study (up to 120 days after surgery). Animals were monitored daily and sacrificed per institutional guidelines when reaching either a Body Conditioning Score of 2 (28) or palpable tumor of 1.5 cm in diameter. Full necropsy was performed at the time of death with snap-frozen and formalin-fixed tissue sections taken of primary and metastatic tumors, as well as normal spleen, lung, liver, small, and large intestine. Histologic analysis was performed with hematoxylin and eosin (H&E)–stained sections by a practicing surgical pathologist (D.W. Dawson) blinded to treatment arms. Ten random high power fields per tumor were analyzed for mitotic counts. A previously described dissemination score awarding points based on tumor infiltration and metastasis (29) was used to quantify tumor spread.

Wnt reporter assays

Dual luciferase assays (Promega) were performed as previously described (7) on cell lines stably transduced with lentiviral constructs containing β-catenin–activated reporter (BAR) driving firefly luciferase expression and separate normalization control construct with constitutive EF1α promoter driving Renilla expression.

Gene knockdown

Lipofectamine 2000 was used per the manufacturer's instructions to transfect AsPC-1 cells with 20 nmol/L control siRNA (#12935-200) or *CTNNB1* s437 (#4390824) siRNA (all purchased from Life Technologies). Western blot analyses to verify knockdown were performed using β-catenin (Sigma; C2206) and tubulin (Santa Cruz; sc-5546) antibodies.

Real-time PCR

RNA extraction, cDNA synthesis, and SYBR Green–based qPCR were performed as previously described (7) using primers listed in Supplementary Table S1.

Downloaded from http://aacrjournals.org/mct/article-pdf/13/10/2303/2327082/2303.pdf by guest on 12 February 2025

Western blot analyses and immunoprecipitation

Western blot analyses were performed as previously described (7) using antibodies specific for β-catenin (Sigma; C2206), PARP [Cell Signaling Technology (CST); 9542], cleaved caspase-3 (CST; 9664), cleaved caspase-7 (CST; 9491), SKP2 (CST; 2652), MYC (Santa Cruz; sc-40), p21 (CST; 2947), or tubulin (Santa Cruz; sc-5546). CBP coimmunoprecipitations were performed on nuclear extracts as previously described (30) with anti-CBP (Santa Cruz; sc-369) or control isotype-matched IgG (Abcam; ab46540) antibodies.

Chromatin immunoprecipitation

AsPC-1 cells (70% confluency) were cross-linked with formalin. Chromatin immunoprecipitation (ChIP) was performed using the Pierce Agarose ChIP Kit (Thermo Scientific) on chromatin digested with 2U micrococcal nuclease. Digested chromatin extracts were precleared with 20 μg agarose beads and incubated overnight with beads prebound with either 5 μg IgG control or CBP antibody (Abcam; ab46540 and ab2832, respectively) blocked with 1 μg fish sperm DNA. PCR was performed using primers (Supplementary Table S1) covering gene regulatory regions for *CDKN1A* (−231 to −117 relative to transcriptional start site, TSS), *SKP2* (1772 to 1870 relative to TSS), and *CDC25A* (−31 to −310 relative to TSS).

Gene expression microarray and data analysis

RNA was extracted from three biologic replicates of AsPC-1 cells 6 and 24 hours after treatment with 10 μmol/L ICG-001 or vehicle control (DMSO) or in separate experiments from two biologic replicates of AsPC1 cells transfected for 48 hours with either 20 nmol/L control or *CTNNB1* siRNA. Affymetrix U133 plus 2.0 oligonucleotide arrays were processed in the UCLA Clinical Microarray Core. Arrays are available in Gene Expression Omnibus database repository (accession code GSE57728). Data analysis was performed with dChip Analysis software package (31) using invariant set normalization and signal intensities summarized using the model-based expression index algorithm with mismatch probe option for background subtraction. Initial gene filtering criteria were set at >10% present call and variance across samples of 0.4 < standard deviation/mean < 1,000. ICG-001–regulated genes were determined by comparative analysis of ICG-001 versus vehicle control (selection criteria >1.67-fold change and $P < 0.01$ at 6 hours or >2-fold change and $P < 0.01$ at 24 hours). β-catenin–regulated genes were determined by comparative analysis of *CTNNB1* versus control siRNA transfection (selection criteria ≥1.33-fold change and >50 absolute change). Functional enrichment was examined using default parameters in the web-based Database for Annotation, Visualization and Integrated Discovery (DAVID, v6.7; http://david.abcc.ncifcrf.gov; ref. 32). Analysis was limited to the gene ontology (GO) biologic process FAT (GOTERM_BP_FAT) category terms and ranked on *P* values after removal of categories with less than 6 annotated genes.

Statistical analysis

Student *t* tests were used to compare continuous variables. The Cox proportional hazard model was used to estimate HRs between treatment groups. The assumption of proportionality was assessed both by visual inspection of Kaplan–Meier survival curves and formal analysis of Schoenfeld residuals ($P = 0.13$). Kaplan–Meier survival curves and log-rank tests were performed using GraphPad Prism.

Results

ICG-001 inhibits *in vitro* PDAC cell line growth

ICG-001 (Fig. 1A) effects on *in vitro* anchorage-dependent PDAC cell growth were addressed by MTT cell viability assays. ICG-001 showed dose-dependent cell growth inhibition of AsPC-1, L3.6pl, PANC-1, and MiaPaCa-2 cell lines at IC_{50} values of 5.48 μmol/L, 14.07 μmol/L, 3.43 μmol/L, and 3.31 μmol/L, respectively (Fig. 1B and Supplementary Fig. S1A and S1B). ICG-001 also significantly inhibited anchorage-independent growth in soft agar assays (Fig. 1C). Addressing the potential for combined use of ICG-001 with cytotoxic chemotherapy, concurrent treatment with 5 μmol/L ICG-001 and 5 nmol/L gemcitabine further increased growth inhibition relative to individual treatments (Fig. 1D).

ICG-001 inhibits *in vivo* PDAC tumor growth

ICG-001 was next addressed in an *in vivo* orthotopic xenograft model of PDAC. AsPC-1 tumor cells were injected into the distal pancreas of nude mice 10 days before the start of treatment. Tumor-bearing mice were then randomized into four different treatment arms, including vehicle ($N = 12$), ICG-001 ($N = 12$), gemcitabine ($N = 11$), or ICG-001 + gemcitabine ($N = 12$). Treatment was continued for a total of 8 weeks, after which all surviving animals were followed until the end of the study (120 days). ICG-001 significantly improved survival compared with vehicle alone as determined by Cox proportional hazard analysis [HR, 0.207; 95% confidence interval (CI), 0.079–0.543; $P = 0.001$]. Gemcitabine also significantly improved survival compared with vehicle (HR, 0.123; 95% CI, 0.045–0.334; $P < 0.001$). There was no survival difference between gemcitabine alone versus ICG-001 alone (HR, 0.592; 95% CI, 0.250–1.399; $P = 0.23$). In line with *in vitro* results, the greatest survival benefit relative to vehicle was seen with combined gemcitabine + ICG-001 (HR, 0.074; 95% CI, 0.026–0.212; $P < 0.001$). Although this combination improved survival relative to ICG-001 alone (HR, 0.360; 95% CI, 0.152–0.848; $P = 0.02$), there was no significant improvement relative to gemcitabine alone (HR, 0.608; 95% CI, 0.254–1.455; $P = 0.66$). Kaplan–Meier survival curves (Fig. 2A) also demonstrated improved survival relative to vehicle control (mean survival, 46 ± 3.1 days) for ICG-001 (mean survival, 64 ± 7.1 days, log-rank $P = 0.01$), gemcitabine (mean survival, 83 ± 5.1 days,

Downloaded from http://aacrjournals.org/mct/article-pdf/13/10/2303/2327082/2303.pdf by guest on 12 February 2025

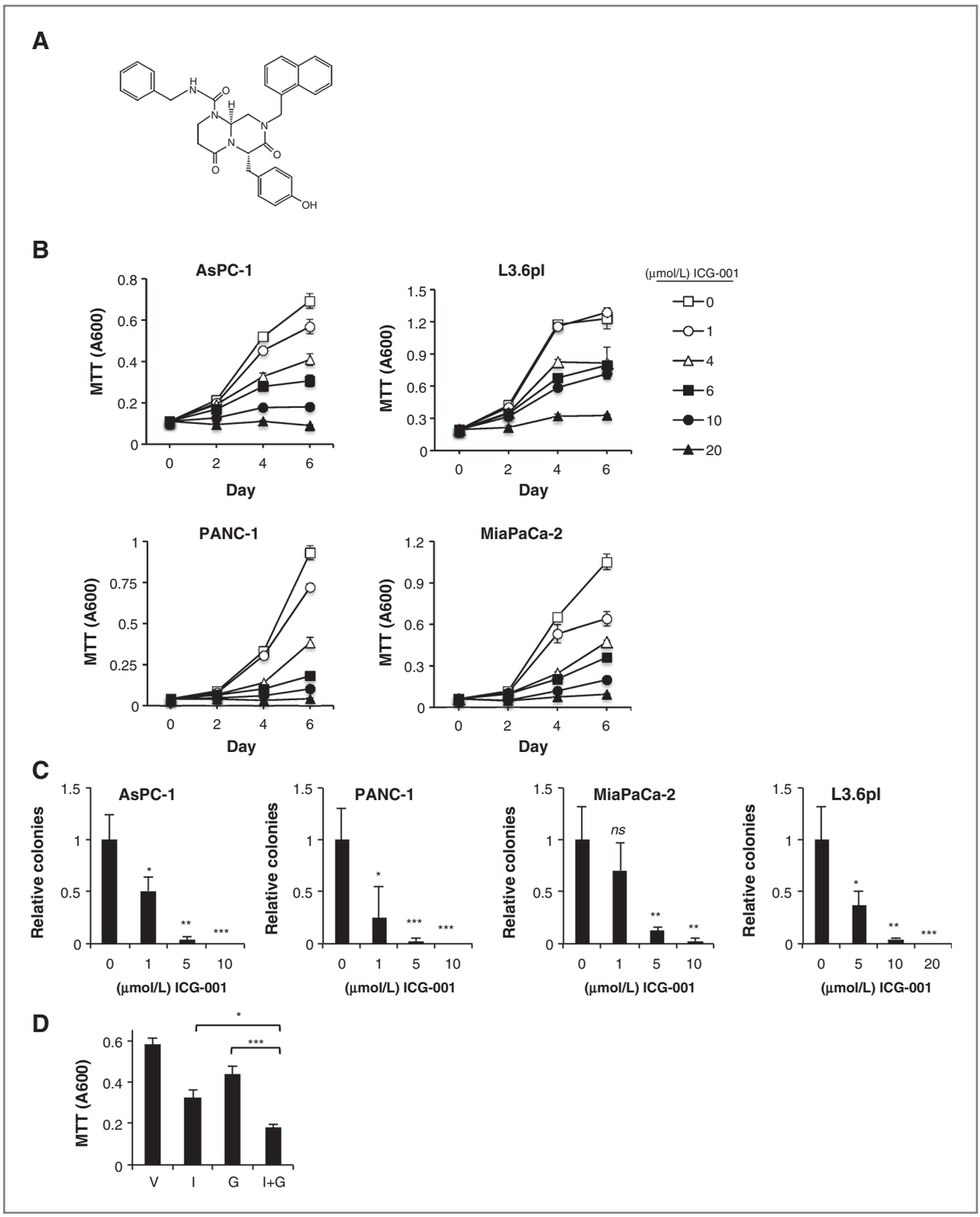

Figure 1. ICG-001 inhibits *in vitro* anchorage-dependent and -independent growth of pancreatic cancer lines. A, chemical structure of ICG-001. MTT cell viability (B) and soft agar assays (C) were performed at the indicated concentrations of ICG-001. D, MTT assay on AsPC-1 cells treated for 6 days with vehicle (V), 5 μmol/L ICG-001 (I), 5 nmol/L gemcitabine (G), or 5 μmol/L ICG-001 plus 5 nmol/L gemcitabine (I + G). Representative experiment from at least three replicates is presented for each cell line. *, $P < 0.05$; **, $P < 0.01$; ***, $P < 0.001$; and ns, not significant.

Downloaded from http://aacrjournals.org/mct/article-pdf/13/10/2303/2327082/2303.pdf by guest on 12 February 2025

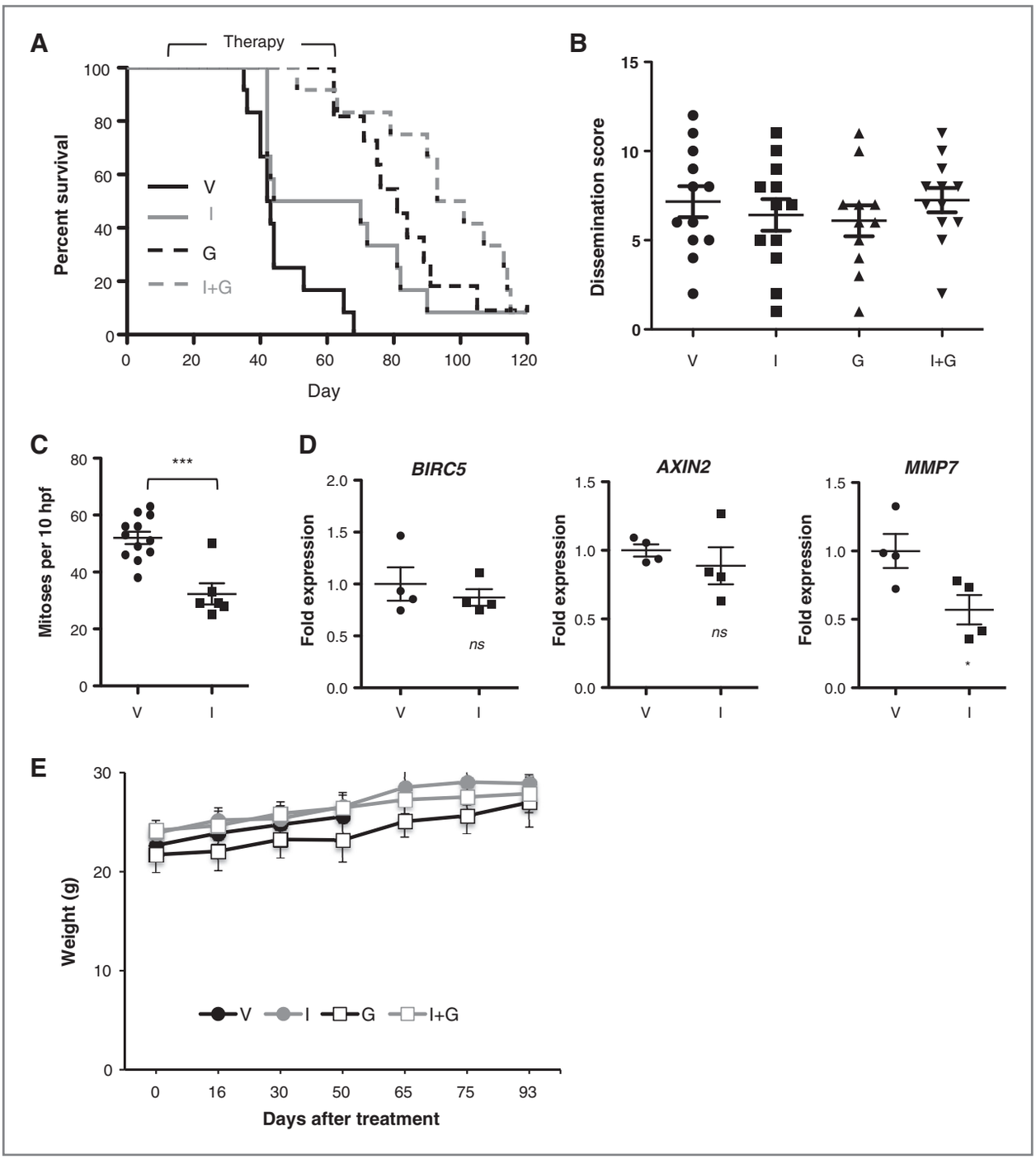

Figure 2. ICG-001 shows *in vivo* efficacy against pancreatic cancer. A, Kaplan–Meier survival curves for mice treated with vehicle (V), ICG-001 (I), gemcitabine (G), or ICG-001 plus gemcitabine (I + G). B, tumor dissemination scores were determined at the time of sacrifice for all mice in the four treatment arms. C, mitotic counts in 10 random high power fields and (D) qPCR analysis of indicated Wnt gene targets normalized to *ACTB* housekeeping gene were determined in primary tumors taken from mice still receiving treatment at time of death. E, weight of mice at various time points following initiation of therapy. *, $P < 0.05$; ***, $P < 0.001$; and ns, not significant.

log-rank $P < 0.00001$), and combined ICG-001 + gemcitabine (mean survival, 95 ± 6.0 days, log-rank $P < 0.00001$) treatments.

The *in vivo* biologic effects of ICG-001 were further addressed by gross and histologic analysis of mice at necropsy. All tumors significantly involved the pancreas

Downloaded from http://aacrjournals.org/mct/article-pdf/13/10/2303/2327082/2303.pdf by guest on 12 February 2025

with direct extension into adjacent spleen. Metastatic tumor deposits were observed in all animals, most frequently involving the lung, small bowel, and diaphragm (Supplementary Fig. S2A–S2F and Supplementary Table S2). Using a previously described scoring system that awards points based on tumor infiltration and metastasis (29), tumor dissemination was quantified at the time of death. No differences were observed between the four treatment arms (Fig. 2B), indicating that animals were reproducibly sacrificed at time points of equal tumor burden. A mitotic index calculated on tumors harvested during drug treatment revealed a significant decrease in mitotic activity in ICG-001 versus vehicle control–treated tumors (Fig. 2C). Real-time qPCR for three well-established Wnt target genes in tumors harvested during drug treatment revealed a significant decrease in *MMP7* expression with ICG-001 versus vehicle control treatment, but no differences in *BIRC5* or *AXIN2* expression (Fig. 2D).

Pharmacologic inhibition of Wnt signaling could have potential deleterious effects on normal somatic stem cell maintenance and tissue homeostasis (26). However, no clinical evidence of ICG-001 cytotoxicity was observed on the basis of body weight measurements (Fig. 2E). Furthermore, H&E evaluation of uninvolved liver and intestine revealed no histologic changes to suggest cytotoxicity in animals sacrificed during treatment with ICG-001 or vehicle control. Small bowel from both treatment groups revealed normal villous:crypt ratios and no changes in apoptotic or mitotic activity within crypts, whereas liver showed no evidence of hepatitis, cholestasis, or hepatocellular injury (i.e., ballooning change or apoptosis; Supplementary Fig. S2G–S2L).

ICG-001 induces G_1 arrest and has variable effects on Wnt/β-catenin signaling

We next explored mechanisms underpinning ICG-001 pancreatic growth inhibitory effects. As previously shown in colorectal cancer (16), ICG-001 disrupted the interaction between CBP and β-catenin in AsPC1 cells as measured by coimmunoprecipitation (Fig. 3A). To examine ICG-001 effects on Wnt/β-catenin signaling, PDAC cell lines stably transduced with a β-catenin–activated luciferase reporter (7, 33) were treated with increasing concentrations of ICG-001. ICG-001 exhibited strong, dose-dependent inhibition of reporter activity in AsPC-1 (Fig. 3B), a cell line characterized by higher levels of autocrine Wnt/β-catenin activity (7). By comparison, high concentrations of ICG-001 only weakly inhibited reporter activity in PANC-1 and

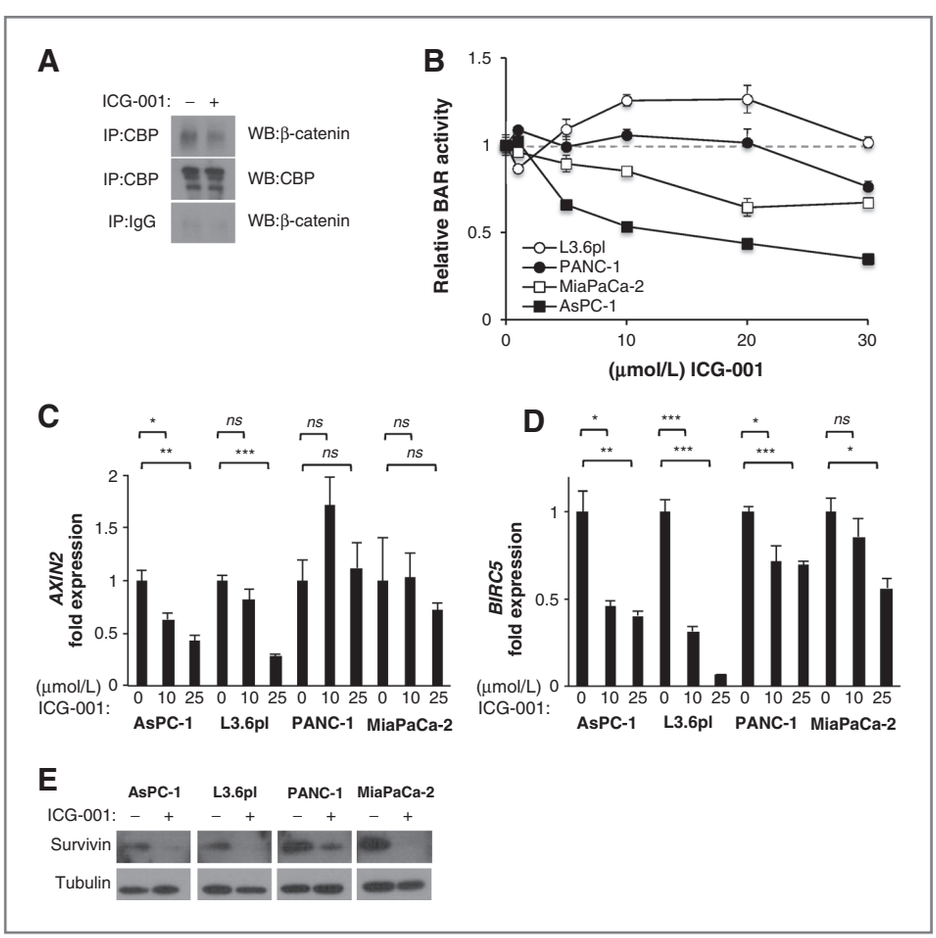

Figure 3. ICG-001 variably influences Wnt transcriptional activity across pancreatic cancer lines. A, nuclear extracts from AsPC-1 cells treated with vehicle or 30 μmol/L ICG-001 for 6 hours were immunoprecipitated with anti-CBP or control IgG antibodies followed by Western blot analyses for β-catenin and CBP. B, PDAC cell lines carrying stably integrated Wnt/β-catenin luciferase reporter (BAR) were treated with indicated concentrations of ICG-001 and measured in dual luciferase reporter assays at 24 hours. Luciferase is normalized to Renilla and shown relative to vehicle. *AXIN2* (C) and *BIRC5* (D) transcript levels were determined by qPCR in PDAC cell lines treated with indicated concentrations of ICG-001. All values were normalized to *ACTB* and shown relative to vehicle. One representative experiment from at least two biologic replicates is shown. E, Western blot for survivin and tubulin (loading control) after 48 hours vehicle or 10 μmol/L ICG-001. One representative experiment of three replicates is shown. *, $P < 0.05$; **, $P < 0.01$; ***, $P < 0.001$; and ns, not significant.

Downloaded from http://aacrjournals.org/mct/article-pdf/13/10/2303/2327082/2303.pdf by guest on 12 February 2025

MiaPaCa-2 cells, and not at all in L3.6pl cells (Fig. 3B). Parallel dose-dependent effects of ICG-001 on the expression of the endogenous Wnt/β-catenin target genes *AXIN2* were also observed, with L3.6pl cells demonstrating disparate inhibition of *AXIN2* expression at high ICG-001 concentration (Fig. 3C). Of note, ICG-001 significantly inhibited the growth of multiple PDAC cell lines at lower concentrations that had little or no effect on Wnt/β-catenin transcriptional activity (compare Fig. 1B and Fig. 3B and C).

ICG-001 has been shown to induce apoptosis via downregulation of the apoptosis inhibitor *BIRC5* (survivin), a known Wnt/β-catenin target gene (16–19). ICG-001 treatment decreased the expression of *BIRC5* transcript and survivin protein levels in all four PDAC cell lines (Fig. 3D and E). Despite this significant inhibition of survivin expression, ICG-001 had no significant effects on AsPC1 apoptosis as determined by cleaved PARP, caspase-3, caspase-7, or Annexin-V–PI flow cytometry (Fig. 4A and B). PANC-1 and MiaPaCa-2 cells showed mild increases in cleaved PARP, caspase-3, and caspase-7 with no appreciable differences in apoptosis by Annexin-V–PI staining, whereas L3.6pl showed significantly increased apoptosis as measured by Annexin-V–PI flow staining (Fig. 4A and B). These modest changes indicated apoptosis was not the primary mechanism for the observed inhibition of PDAC growth by ICG-001. Therefore, ICG-001 effects on cell proliferation were analyzed by cell-cycle analysis. ICG-001 treatment robustly induced G_1 arrest in all PDAC cell lines (Fig. 4C), a finding consistent with the decreased mitotic activity observed in ICG-001–treated orthotopic tumors (Fig. 2C). Significant G_1 arrest was observed in all four cell lines at 10 μmol/L ICG-001, a concentration for which only AsPC-1 showed appreciable inhibition of Wnt transcriptional activity.

If ICG-001 exerts antiproliferative effects by inhibiting β-catenin–mediated transcription, this effect should be phenocopied by knockdown of β-catenin expression. However, siRNA-mediated *CTNNB1* gene knockdown failed to induce G_1 arrest in AsPC-1 cells, whereas parallel ICG-001 treatment did induce significant G_1 arrest (Fig. 4D). Furthermore, although exogenous Wnt3A ligand treatment fully rescued ICG-001 inhibition of Wnt reporter activity in the cell lines, it had no effect on ICG-001–mediated G_1 cell-cycle arrest (Supplementary Fig. S3). Altogether, these data indicate that ICG-001 mediates growth arrest in PDAC cell lines through mechanisms discrete from its action as an inhibitor of Wnt signaling.

ICG-001 inhibits the expression of genes involved in cell cycle

To explore mechanisms underlying ICG-001 inhibition of cell cycle in PDAC, gene expression microarrays were performed on AsPC-1 cells after 6 and 24 hours of treatment with ICG-001. In total, 569 transcripts (419 upregulated and 150 downregulated) showed altered expression

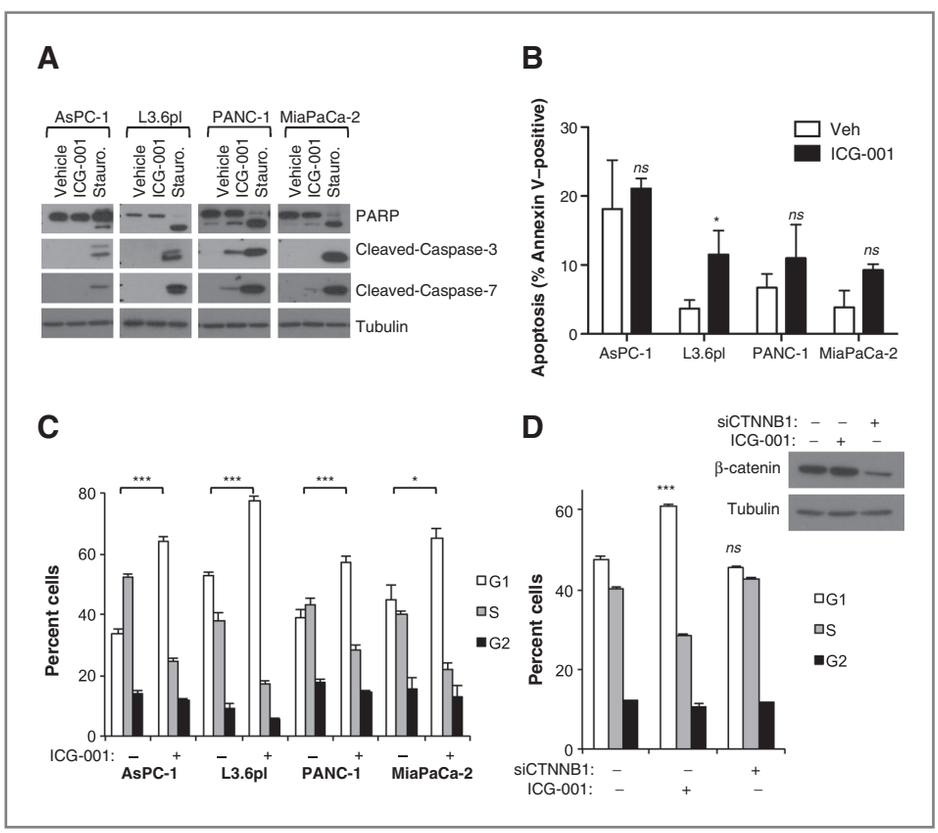

Figure 4. ICG-001 robustly induces G_1 cell-cycle arrest. A, cells were incubated with vehicle, 10 μmol/L ICG-001, or 500 nmol/L staurosporine (Stauro, positive control for apoptosis) for 24 hours and analyzed by Western blot for PARP, cleaved-caspase-3, cleaved-caspase-7, and tubulin (loading control). Vehicle or 10 μmol/L ICG-001–treated cells were analyzed by flow cytometry for (B) apoptosis by Annexin-V–PI staining at 48 hours or (C) cell cycle by PI staining at 24 hours. D, cell-cycle analysis was determined for AsPC-1 cells treated simultaneously with indicated combinations of vehicle, 10 μmol/L ICG-001, control siRNA (20 nmol/L), or CTNNB1 siRNA (20 nmol/L) for 48 hours. Western blot confirmed >75% knockdown of β-catenin with CTNNB1 siRNA. One representative experiment of three replicates is shown for all figures. *, $P < 0.05$; ***, $P < 0.001$; and ns, not significant.

Downloaded from http://aacrjournals.org/mct/article-pdf/13/10/2303/2327082/2303.pdf by guest on 12 February 2025

in response to ICG-001 treatment ($P < 0.01$; 1.67-fold change at 6 hours or 2-fold change at 24 hours; 0.2% median false discovery rate; Fig. 5A; and Supplementary Table S3). Several of these changes were further validated by qPCR in separate ICG-001 treatment experiments (Fig. 5B). To explore biologic processes linked to ICG-001 treatment, we performed enrichment analysis of GO functional annotations. In line with phenotypic observations, the top five GO terms for genes downregulated by ICG-001 were DNA replication, DNA metabolic processes, DNA replication initiation, DNA-dependent DNA replication, and cell cycle ($P < 0.00013$; Supplementary Fig. S4A). Top GO terms for genes upregulated by ICG-001 included multicellular organismal homeostasis, negative regulation of cell proliferation, cell-cycle arrest, regulation of angiogenesis, and regulation of cell proliferation ($P < 0.001$; Supplementary Fig. S4B).

Although its inhibition of PDAC cell proliferation did not seem mechanistically linked to its effects on Wnt/β-catenin transcriptional activity, ICG-001 did inhibit several known Wnt transcriptional targets, including *MMP7* and *LGR5* that were further validated by qPCR (Fig. 5B). To address ICG-001–regulated genes representing actual Wnt transcriptional targets in PDAC, we compared ICG-001 results with a second microarray study comparing gene expression changes in AsPC-1 transfected with either control or *CTNNB1* siRNA. In the context of greater than 80% *CTNNB1* knockdown, there were 441 altered transcripts (absolute fold change ≥ 1.33; median false discovery rate 10.4%), including 228 upregulated and 213 downregulated genes (Supplementary Table S3). Top GO terms for genes downregulated by *CTNNB1* knockdown included cell fate commitment, tube morphogenesis, tube development, morphogenesis of a branching structure, and angiogenesis ($P < 0.0005$; Supplementary Fig. S5A). Top GO terms for genes upregulated by *CTNNB1* siRNA included response to wounding, cell adhesion, biologic adhesion, response to inorganic substance, and regulation of cell migration ($P < 0.0002$; Supplementary Fig. S5B). Cross-referencing both ICG-001 and *CTNNB1* siRNA microarray results revealed 117 overlapping transcripts (Fig. 5C; Supplementary Table S3). GO functional annotations were only marginally enriched in this overlapping dataset ($P < 0.01$), but included regulation of cell proliferation, positive regulation of developmental processes, homeostatic process, response to wounding, and regulation of the cell cycle.

Among the most highly regulated genes identified in the ICG-001 arrays were *SKP2*, *CDC25A*, and *CDKN1A* (p21), each regulators of cell-cycle progression. We

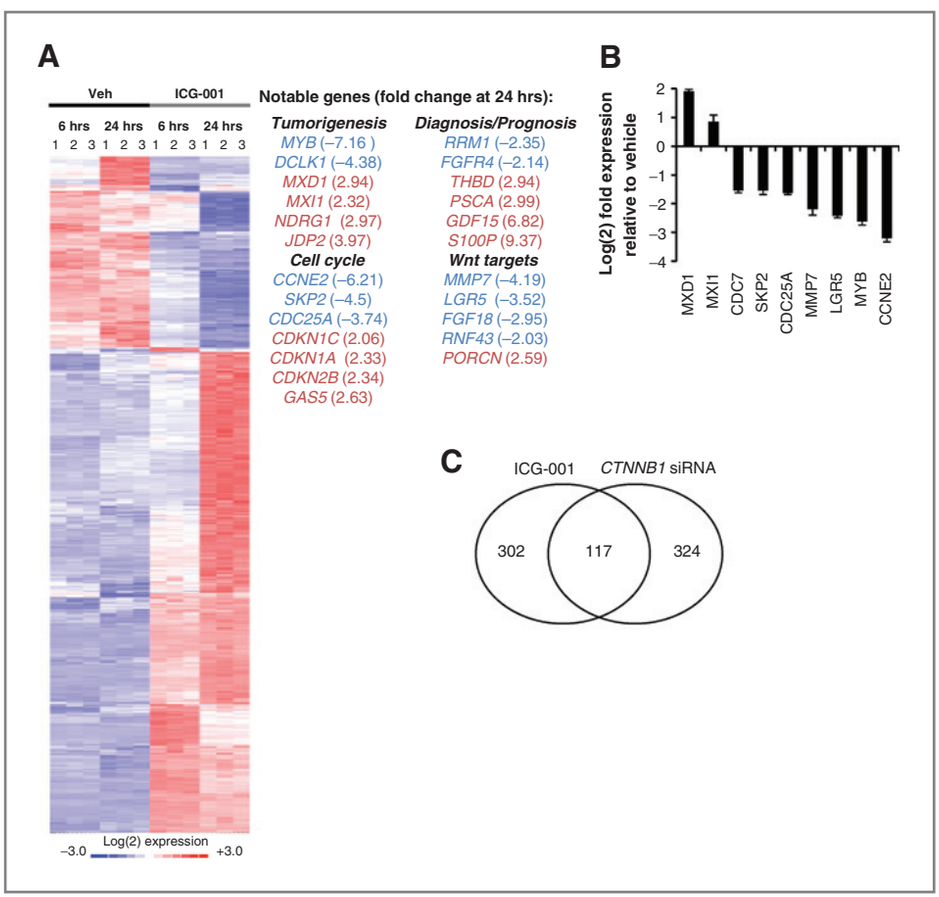

Figure 5. ICG-001 alters the expression of cell-cycle genes. A, gene expression was determined with Affymetrix Human U133 plus 2.0 microarrays using RNA collected from AsPC1 following 6 or 24 hour treatment with vehicle or 10 μmol/L ICG-001. Biologic replicates of significantly regulated genes are shown in the heatmap along with a partial list of genes curated based on known roles in tumorigenesis, cell-cycle control, cancer diagnosis/prognosis, or Wnt/β-catenin transcriptional targets. B, qPCR validation was performed on selected genes in AsPC-1 cells separately treated with vehicle or 10 μmol/L ICG-001 for 24 hours. C, Venn diagram comparing AsPC-1 gene expression microarray changes observed with either 10 μmol/L ICG-001 treatment or *CTNNB1* siRNA transfection.

Downloaded from http://aacrjournals.org/mct/article-pdf/13/10/2303/2327082/2303.pdf by guest on 12 February 2025

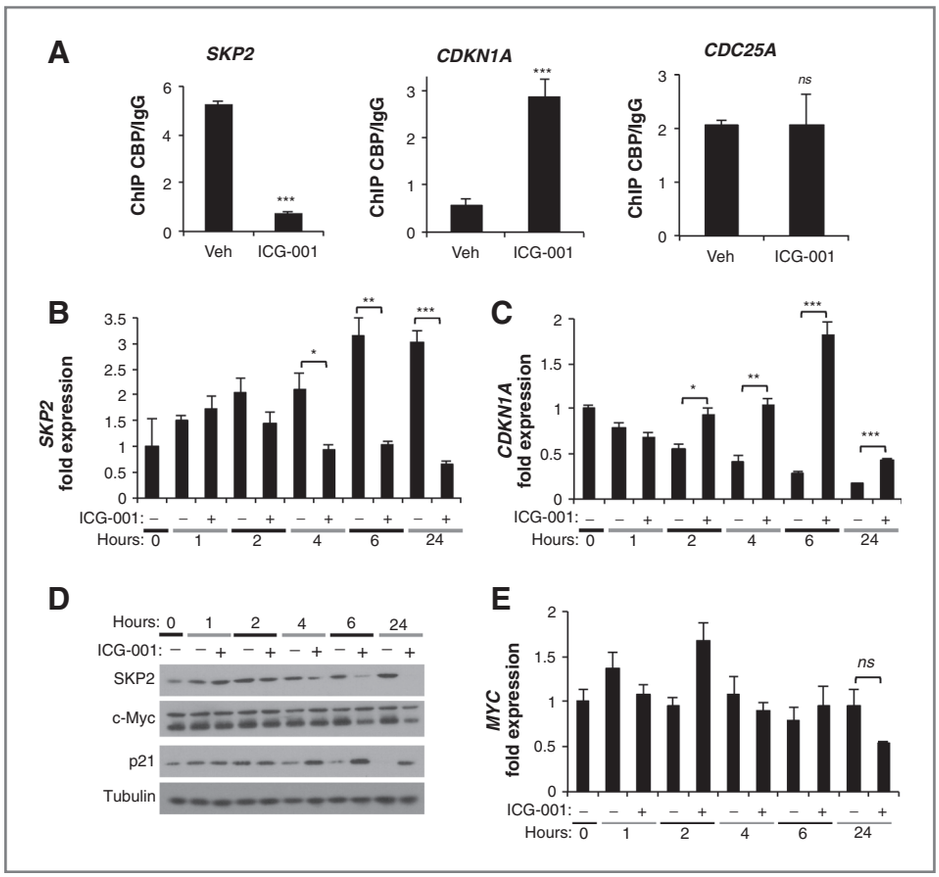

Figure 6. ICG-001 directly regulates change in *SKP2* and *CDKN1A* expression. A, ChIP results for CBP association with *SKP2*, *CDKN1A*, and *CDC25A* regulatory elements in AsPC-1 cells following 1 hour treatment with vehicle or 10 μmol/L ICG-001. Data were normalized to input DNA and are presented as fold change of CBP/IgG. Representative experiments of three replicates are shown. B–E, time-course study of AsPC-1 cells treated with vehicle or 10 μmol/L ICG-001 measuring *SKP2* (B) and *CDKN1A* (C) gene expression by qPCR; SKP2, MYC, p21, and tubulin protein expression by Western blot (D); and *MYC* gene expression by qPCR (E). All qPCR values were normalized to ACTB and shown relative to 0 hour. Representative experiments from at least two replicates are shown for all qPCR and Western blot analyses. *, $P < 0.05$; **, $P < 0.01$; ***, $P < 0.001$; and ns, not significant.

therefore explored whether these genes were direct transcriptional targets of CBP that are altered in response to ICG-001 treatment. After 1-hour ICG-001 treatment, ChIP revealed reduced CBP occupancy at *SKP2* and increased CBP occupancy at *CDKN1A* (Fig. 6A), corresponding, respectively, to aforementioned decreased *SKP2* and increased *CDKN1A* gene expression results (Fig. 5). No change in CBP occupancy was observed at *CDC25A* (Fig. 6A), suggesting that it is transcriptionally downregulated indirectly in response to ICG-001. Further detailed time-course analyses of gene and protein expression revealed *SKP2* transcript levels were reduced within 4 hours, whereas *CDKN1A* transcript levels were increased within 2 hours of ICG-001 treatment (Fig. 6B and C). Corresponding decrease in SKP2 protein expression and increase in p21 protein expression were observed within 4 to 6 hours of ICG-001 treatment (Fig. 6D). MYC protein levels were also decreased after 6 hours, although *MYC* transcript levels were unchanged (Fig. 6D and E), indicating that a posttranscriptional mechanism controls MYC protein levels following ICG-001 treatment.

Discussion

At least subsets of PDAC are dependent upon Wnt/β-catenin signaling for initiation and/or progression (6–10, 34), warranting exploration of ICG-001 and other Wnt inhibitors as potential therapeutics. PRI-724, an ICG-001 derivative, is presently under investigation in combination with gemcitabine in a phase I clinical trial for patients with metastatic pancreatic cancer (NCT01764477). We have demonstrated that ICG-001 significantly inhibits *in vitro* PDAC growth through induction of G_1 cell-cycle arrest and improves survival in an *in vivo* orthotopic xenograft model of PDAC. Despite augmented PDAC growth inhibition *in vitro*, combined ICG-001 and gemcitabine did not further improve survival over gemcitabine alone in the xenograft model. It is possible that robust induction of G_1 arrest with ICG-001 compromises the action of cytotoxic chemotherapy such as gemcitabine, which primarily kills cancer cells undergoing DNA synthesis in S phase. An analogous situation has been observed with CDK4 inhibitors that by inducing G_1 arrest can reduce the efficacy of cytotoxic chemotherapy in certain circumstances (35). Further optimization of the dosing and delivery of ICG-001 (or PRI-724) is needed to resolve whether ICG-001 can be used effectively in combination with gemcitabine. Intriguingly, ICG-001 reduced expression of *RRM1* in AsPC-1 microarrays. *RRM1* expression directly correlates with gemcitabine resistance (36) and worse overall survival in PDAC (37, 38). Furthermore, ICG-001 was shown to act synergistically with

Downloaded from http://aacrjournals.org/mct/article-pdf/13/10/2303/2327082/2303.pdf by guest on 12 February 2025

conventional chemotherapy to prolong survival in NOD/SCID mice engrafted with primary acute lymphoblastic leukemia (22). Thus, optimized combinations of cytotoxic regimens with ICG-001 may still offer additional survival benefit in PDAC or other tumors.

ICG-001 treatment and β-catenin knockdown regulated an overlapping set of genes in AsPC-1, including known targets of canonical Wnt signaling (i.e., *MMP7, EDN1, LGR5, RNF43*, and *PORCN*). Originally identified in a small-molecule library screen of compounds that inhibited β-catenin/T-cell factor (TCF)–dependent reporter activity, ICG-001 inhibits Wnt transcriptional activity by binding to the N-terminal domain of CBP and preventing its interaction with β-catenin (16). This not only has the potential to disrupt CBP-dependent β-catenin–TCF transcription, but also may increase the pool of β-catenin available to interact with p300. Like CBP, p300 functions either as a transcriptional coactivator or corepressor in a context-dependent manner (26, 39, 40). Kahn and colleagues have proposed a model of CBP/p300 differential coactivator usage whereby TCF–β-catenin–CBP-mediated transcription drives a nondifferentiated proliferative state with ICG-001 inducing a switch to TCF–β-catenin–p300-mediated transcription favoring cellular differentiation (39, 41). In keeping with this model, ICG-001 strongly induced G_1 cell-cycle arrest in PDAC cell lines and inhibited the expression of certain genes linked to pluripotency, including *LGR5* that marks progenitor cells in intestinal crypts and *DCLK1* which was recently shown to mark a unique tumor initiating cell population in PDAC (42). ICG-001 also regulated many genes unaltered by β-catenin knockdown, including several linked to DNA replication and cell-cycle regulation. Beyond β-catenin, ICG-001 could more generally alter gene expression by disrupting CBP interaction with any of a number of other known protein binding partners that includes many transcription factors (43). As an example, ICG-001 was recently shown to block CBP binding to γ-catenin, resulting in increased p300/γ-catenin interaction and decreased *BIRC5* expression (22, 44).

ICG-001 can induce caspase-3/7–mediated apoptosis in colon cancer cells via downregulation of *BIRC5* (16). Although ICG-001 treatment inhibited survivin protein levels, there were only variable and modest effects on apoptosis in PDAC cell lines. Rather, ICG-001 induced robust G_1 cell-cycle arrest, which is perhaps not unexpected given CBP/p300 histone acetyltransferase activity is essential for cell proliferation and orderly G_1–S transition (45). Several groups find that Wnt/β-catenin signaling promotes cellular proliferation in PDAC (4, 9) and while Wnt/β-catenin transcriptional targets *MYC* or *CCND1* are commonly linked to its regulation of the cell cycle, transcript levels of these genes were not altered in PDAC cell lines in response to ICG-001 treatment. Moreover, growth inhibition and G_1 cell-cycle arrest were observed in multiple PDAC cell lines at ICG-001 concentrations with little or no measurable effect on Wnt reporter activity or endogenous *AXIN2* expression, indicating ICG-001 inhibition of PDAC cell proliferation was decoupled from its function as a Wnt inhibitor.

ICG-001 treatment altered the expression of numerous genes linked to DNA replication and cell cycle in AsPC-1 microarray analysis, both downregulating genes that promote (i.e., *SKP2, CDC25A, CDC7, CCNE*, and *MCM2-MCM 6*) and upregulating genes that inhibit (i.e., *CDKN1A, CDKN1C, CDKN2B, MXD1, MXI1*, and *BTG1*) cell-cycle progression. ICG-001 induced rapid changes in CBP occupancy on *SKP2* and *CDKN1A* regulatory regions with corresponding changes in mRNA and protein levels, implicating *SKP2* and *CDKN1A* as direct targets of ICG-001–mediated cell-cycle arrest. SKP2 is a substrate component of the SCF E3 ubiquitin-protein ligase complex that promotes cell-cycle progression through ubiquitination and subsequent degradation of several proteins linked to cell-cycle inhibition, including p21, p27, p57, p130, and RASSF1A among others (46). ICG-001 increased CBP occupancy at *CDKN1A* promoter site in AsPC-1 cells, perhaps by increasing the availability of CBP to different subsets of transcription factors mediating *CDKN1A* expression. *CDKN1A* encodes the cyclin-dependent kinase inhibitor p21 that opposes the function of multiple cyclin–CDK complexes that mediate G_1 and S cell-cycle progression. Increased p21 levels with ICG-001 could reflect decreased SKP2-mediated degradation of p21 and/or increased *CDKN1A* expression via CBP cotranscriptional activation. Although *MYC* transcript levels were unchanged, ICG-001 reduced MYC protein levels within 6 hours along with corresponding increases in several known targets of MYC-mediated transcriptional repression (i.e., *CDKN1A, CDKN1C*, and *CDKN2B*). It is intriguing to speculate how ICG-001 might indirectly antagonize MYC through additional posttranslational mechanisms linked to its protein stability or function. *MXD1* and *MXI1*, which were both upregulated in response to ICG-001 treatment, can inhibit the transcriptional activity of MYC by competing for its important heterodimerization partner MAX (47). CBP/p300-mediated acetylation has been shown to stabilize MYC protein and function (48), which could also be perturbed by ICG-001. Finally, ICG-001 could indirectly disrupt MYC activity through its aforementioned downregulation of SKP2, which has been shown to ubiquitylate MYC to license its function as a transcriptional activator (49).

In conclusion, ICG-001 seems to robustly inhibit PDAC growth through both direct and indirect mechanisms that mutually reinforce the induction of G_1 cell-cycle arrest. Although further studies are needed to expand upon precise mechanisms underpinning its transcriptional and phenotypic activities, ICG-001 seems to more broadly disrupt CBP function beyond its effects as cotranscriptional activator of Wnt/β-catenin signaling. These future studies should not only further examine the therapeutic potential of ICG-001 and its derivatives in PDAC or other cancers, but also better establish effective drug combinations and patient selection.

Downloaded from http://aacrjournals.org/mct/article-pdf/13/10/2303/2327082/2303.pdf by guest on 12 February 2025

Disclosure of Potential Conflicts of Interest

No potential conflicts of interest were disclosed.

Authors' Contributions

Conception and design: M.D. Arensman, T.R. Donahue, D.W. Dawson
Development of methodology: M.D. Arensman, T.R. Donahue, D.W. Dawson
Acquisition of data (provided animals, acquired and managed patients, provided facilities, etc.): M.D. Arensman, A.R. Lay, K.M. Kershaw, N. Wu, T.R. Donahue, D.W. Dawson
Analysis and interpretation of data (e.g., statistical analysis, biostatistics, computational analysis): M.D. Arensman, D. Telesca, A.R. Lay, K.M. Kershaw, N. Wu, T.R. Donahue, D.W. Dawson
Writing, review, and/or revision of the manuscript: M.D. Arensman, T.R. Donahue, D.W. Dawson
Administrative, technical, or material support (i.e., reporting or organizing data, constructing databases): M.D. Arensman, D.W. Dawson
Study supervision: M.D. Arensman, D.W. Dawson

Grant Support

M.D. Arensman was supported by USHHS Ruth L. Kirschstein Institutional National Research Service Award #T32 CA009056 (UCLA Tumor Biology Training Grant). D.W. Dawson was supported by an American Cancer Society Research Scholars Grant (RSG-12-083-01-TBG), NIH (P01 CA163200), and the Hirshberg Foundation for Pancreatic Cancer Research. Flow cytometry was performed in the UCLA Jonsson Comprehensive Cancer Center (JCCC) and Center for AIDS Research Flow Cytometry Core Facility supported by NIH awards CA-16042 and AI-28697, and by the JCCC, UCLA AIDS Institute, and David Geffen School of Medicine at UCLA.

The costs of publication of this article were defrayed in part by the payment of page charges. This article must therefore be hereby marked *advertisement* in accordance with 18 U.S.C. Section 1734 solely to indicate this fact.

Received November 22, 2013; revised July 9, 2014; accepted July 12, 2014; published OnlineFirst July 31, 2014.

References

1. Siegel R, Naishadham D, Jemal A. Cancer statistics, 2012. CA Cancer J Clin 2012;62:10–29.
2. Vincent A, Herman J, Schulick R, Hruban RH, Goggins M. Pancreatic cancer. Lancet 2011;378:607–20.
3. Clevers H. Wnt/beta-catenin signaling in development and disease. Cell 2006;127:469–80.
4. Morris JP, Wang SC, Hebrok M. KRAS, Hedgehog, Wnt and the twisted developmental biology of pancreatic ductal adenocarcinoma. Nat Rev Cancer 2010;10:683–95.
5. White BD, Chien AJ, Dawson DW. Dysregulation of Wnt/β-catenin signaling in gastrointestinal cancers. Gastroenterology 2011;142:219–32.
6. Zhang Y, Morris JP, Yan W, Schofield HK, Gurney A, Simeone DM, et al. Canonical wnt signaling is required for pancreatic carcinogenesis. Cancer Res 2013;73:4909–22.
7. Arensman MD, Kovochich a N, Kulikauskas RM, Lay a R, Yang P-T, Li X, et al. WNT7B mediates autocrine Wnt/β-catenin signaling and anchorage-independent growth in pancreatic adenocarcinoma. Oncogene 2014;33:899–908.
8. Zeng G, Germinaro M, Micsenyi A, Monga NK, Bell A, Sood A, et al. Aberrant Wnt/beta-catenin signaling in pancreatic adenocarcinoma. Neoplasia 2006;8:279–89.
9. Pasca di Magliano M, Biankin A V, Heiser PW, Cano D a, Gutierrez PJ a, Deramaudt T, et al. Common activation of canonical Wnt signaling in pancreatic adenocarcinoma. PLoS One 2007;2:1–9.
10. Wang L, Heidt DG, Lee CJ, Yang H, Logsdon CD, Zhang L, et al. Oncogenic function of ATDC in pancreatic cancer through Wnt pathway activation and beta-catenin stabilization. Cancer Cell 2009;15:207–19.
11. Froeling FEM, Feig C, Chelala C, Dobson R, Mein CE, Tuveson D a, et al. Retinoic acid-induced pancreatic stellate cell quiescence reduces paracrine Wnt-β-catenin signaling to slow tumor progression. Gastroenterology 2011;141:1486–97.
12. Jiang X, Hao H-X, Growney JD, Woolfenden S, Bottiglio C, Ng N, et al. Inactivating mutations of RNF43 confer Wnt dependency in pancreatic ductal adenocarcinoma. Proc Natl Acad Sci U S A 2013;110:12649–54.
13. Gurney A, Axelrod F, Bond CJ, Cain J, Chartier C, Donigan L, et al. Wnt pathway inhibition via the targeting of Frizzled receptors results in decreased growth and tumorigenicity of human tumors. Proc Natl Acad Sci U S A 2012;109:11717–22.
14. Voronkov A, Krauss S. Wnt/beta-catenin signaling and small molecule inhibitors. Curr Pharm Des 2013;19:634–64.
15. Anastas JN, Moon RT. WNT signalling pathways as therapeutic targets in cancer. Nat Rev Cancer 2013;13:11–26.
16. Emami KH, Nguyen C, Ma H, Kim DH, Jeong KW, Eguchi M, et al. A small molecule inhibitor of beta-catenin/CREB-binding protein transcription [corrected]. Proc Natl Acad Sci U S A 2004;101:12682–7.
17. Lazarova DL, Chiaro C, Wong T, Drago E, Rainey A, O'Malley S, et al. CBP activity mediates effects of the histone deacetylase inhibitor butyrate on WNT activity and apoptosis in colon cancer cells. J Cancer 2013;4:481–90.
18. Lazarova DL, Wong T, Chiaro C, Drago E, Bordonaro M. p300 influences butyrate-mediated WNT hyperactivation in colorectal cancer cells. J Cancer 2013;4:491–501.
19. Ma H, Nguyen C, Lee K-S, Kahn M. Differential roles for the coactivators CBP and p300 on TCF/beta-catenin-mediated survivin gene expression. Oncogene 2005;24:3619–31.
20. Henderson WR, Chi EY, Ye X, Nguyen C, Tien Y, Zhou B, et al. Inhibition of Wnt/beta-catenin/CREB binding protein (CBP) signaling reverses pulmonary fibrosis. Proc Natl Acad Sci U S A 2010;107:14309–14.
21. Hao S, He W, Li Y, Ding H, Hou Y, Nie J, et al. Targeted inhibition of β-catenin/CBP signaling ameliorates renal interstitial fibrosis. J Am Soc Nephrol 2011;22:1642–53.
22. Gang EJ, Hsieh Y-T, Pham J, Zhao Y, Nguyen C, Huantes S, et al. Small-molecule inhibition of CBP/catenin interactions eliminates drug-resistant clones in acute lymphoblastic leukemia. Oncogene 2014;33:2169–78.
23. Sasaki T, Hwang H, Nguyen C, Kloner RA, Kahn M. The small molecule Wnt signaling modulator ICG-001 improves contractile function in chronically infarcted rat myocardium. PLoS One 2013;8:e75010.
24. Beyer C, Reichert H, Akan H, Mallano T, Schramm A, Dees C, et al. Blockade of canonical Wnt signalling ameliorates experimental dermal fibrosis. Ann Rheum Dis 2013;72:1255–8.
25. Wend P, Fang L, Zhu Q, Schipper JH, Loddenkemper C, Kosel F, et al. Wnt/β-catenin signalling induces MLL to create epigenetic changes in salivary gland tumours. EMBO J 2013;32:1977–89.
26. Takahashi-Yanaga F, Kahn M. Targeting Wnt signaling: can we safely eradicate cancer stem cells? Clin Cancer Res 2010;16:3153–62.
27. Kim MP, Evans DB, Wang H, Abbruzzese JL, Fleming JB, Gallick GE. Generation of orthotopic and heterotopic human pancreatic cancer xenografts in immunodeficient mice. Nat Protoc 2009;4:1670–80.
28. Foltz C, Ullman-Cullere M. Guidelines for assessing the health and condition of mice. Lab Anim (NY) 1999;28:28–32.
29. Hotz HG, Reber HA, Hotz B, Yu T, Foitzik T, Buhr HJ, et al. An orthotopic nude mouse model for evaluating pathophysiology and therapy of pancreatic cancer. Pancreas 2003;26.
30. Guo R, Xu D, Wang W. Identification and analysis of new proteins involved in the DNA damage response network of Fanconi anemia and Bloom syndrome. Methods 2009;48:72–9.
31. Li C, Wong WH. Model-based analysis of oligonucleotide arrays: expression index computation and outlier detection. Proc Natl Acad Sci U S A 2001;98:31–6.
32. Huang DW, Sherman BT, Lempicki RA. Systematic and integrative analysis of large gene lists using DAVID bioinformatics resources. Nat Protoc 2009;4:44–57.

Downloaded from http://aacrjournals.org/mct/article-pdf/13/10/2303/2327082/2303.pdf by guest on 12 February 2025

33. Biechele TL, Moon RT. Assaying beta-catenin/TCF transcription with beta-catenin/TCF transcription-based reporter constructs. Methods Mol Biol 2008;468:99–110.
34. Yu M, Ting DT, Stott SL, Wittner BS, Ozsolak F, Paul S, et al. RNA sequencing of pancreatic circulating tumour cells implicates WNT signalling in metastasis. Nature 2012;487:510–3.
35. Dickson MA. Molecular pathways: CDK4 inhibitors for cancer therapy. Clin Cancer Res 2014;20:3379–83.
36. Mini E, Nobili S, Caciagli B, Landini I, Mazzei T. Cellular pharmacology of gemcitabine. Ann Oncol 2006;17:v7–12.
37. Xie H, Jiang W, Jiang J, Wang Y, Kim R, Liu X, et al. Predictive and prognostic roles of ribonucleotide reductase M1 in resectable pancreatic adenocarcinoma. Cancer 2013;119:173–81.
38. Wei CH, Gorgan TR, Elashoff DA, Hines OJ, Farrell JJ, Donahue TR. A meta-analysis of gemcitabine biomarkers in patients with pancreaticobiliary cancers. Pancreas 2013;42:1303–10.
39. McMillan M, Kahn M. Investigating Wnt signaling: a chemogenomic safari. Drug Discov Today 2005;10:1467–74.
40. Kahn M. Symmetric division versus asymmetric division: a tale of two coactivators. Future Med Chem 2011;3:1745–63.
41. Miyabayashi T, Teo J, Yamamoto M, Mcmillan M, Nguyen C, Kahn M. Wnt/-catenin/CBP signaling maintains long-term murine embryonic stem cell pluripotency. Proc Natl Acad Sci 2007;104: 5668–73.
42. Bailey JM, Alsina J, Rasheed Z a, McAllister FM, Fu Y-Y, Plentz R, et al. DCLK1 marks a morphologically distinct subpopulation of cells with stem cell properties in pre-invasive pancreatic cancer. Gastroenterology 2014;146:245–56.
43. Goodman RH, Smolik S. CBP/p300 in cell growth, transformation, and development. Genes Dev 2000;14:1553–77.
44. Kim Y-M, Ma H, Oehler VG, Gang EJ, Nguyen C, Masiello D, et al. The gamma catenin/CBP complex maintains survivin transcription in β-catenin deficient/depleted cancer cells. Curr Cancer Drug Targets 2011;11:213–25.
45. Ait-Si-Ali S, Polesskaya a, Filleur S, Ferreira R, Duquet a, Robin P, et al. CBP/p300 histone acetyl-transferase activity is important for the G1/S transition. Oncogene 2000;19:2430–7.
46. Chan C-H, Lee S-W, Wang J, Lin H-K. Regulation of Skp2 expression and activity and its role in cancer progression. Sci World J 2010;10:1001–15.
47. Hurlin PJ, Huang J. The MAX-interacting transcription factor network. Semin Cancer Biol 2006;16:265–74.
48. Faiola F, Liu X, Lo S, Pan S, Zhang K, Lymar E, et al. Dual regulation of MYC by p300 via acetylation-dependent control of myc protein turnover and coactivation of myc-induced transcription. Mol Cell Biol 2005;25:10220–34.
49. Jin J, Harper JW. A license to kill: transcriptional activation and enhanced turnover of Myc by the SCF(kp2) ubiquitin ligase. Cancer Cell 2003;3:517–8.

Downloaded from http://aacrjournals.org/mct/article-pdf/13/10/2303/2327082/2303.pdf by guest on 12 February 2025